

# HEAT TRANSFER COEFFICIENT FOR TURBULENT FLOW IN A POROUS MEDIUM FORMED BY A TRIANGULAR ARRAY OF SQUARE RODS

Marcelo B. Saito

Marcelo J.S. De-Lemos<sup>1</sup>

Departamento de Energia - IEME

Instituto Tecnológico de Aeronáutica - ITA

12228-900 - São José dos Campos - SP - Brasil

<sup>1</sup> Corresponding author, delemos@ita.br.

**Abstract.** *Interfacial heat transfer coefficients in a porous medium modeled as a staggered array of square rods are numerically determined. High and low Reynolds  $k$ - $\epsilon$  turbulence models are used in conjunction of a two-energy equation model, which includes distinct transport equations for the fluid and the solid phases. The literature has documented proposals for macroscopic energy equation modeling for porous media considering the local thermal equilibrium hypothesis and laminar flow. In addition, two-energy equation models have been proposed for conduction and laminar convection in packed beds. With the aim of contributing to new developments, this work treats turbulent heat transport modeling in porous media under the local thermal non-equilibrium assumption. Macroscopic time average equations for continuity, momentum, and energy are presented based on the recently established double decomposition concept (spatial deviations and temporal fluctuations of flow properties). The numerical technique employed for discretizing the governing equations is the control volume method. Turbulent flow results for the macroscopic heat transfer coefficient, between the fluid and solid phase in a periodic cell, are presented.*

**Keywords.** *Porous Media, Heat Transfer Coefficient, Thermal Non-Equilibrium.*

## 1. Introduction

The present investigation is concerned with the modeling of heat transfer in a porous medium which the solid material consists of square rods, or alternatively in which the pore space consist of square tubes, in a situation in which local equilibrium is not valid. The wide applications available have led to numerous investigations in this area. Such applications can be found in electronic cooling, heat pipes, nuclear reactors, drying technology, multiphase catalytic reactors and others. The use of two-equation model is required for these types of problems. Kuwahara et al. (2001) proposed a numerical procedure to determine macroscopic transport coefficients from a theoretical basis without any empiricism. They used a single unit cell and determined the interfacial heat transfer coefficient for the asymptotic case of infinite conductivity of the solid phase. Nakayama et al. (2001) extended the conduction model of Hsu (1999) for treating also convection in porous media. Having established the macroscopic energy equations for both phases, useful exact solutions were obtained for two fundamental heat transfer processes associated with porous media, namely, steady conduction in a porous slab with internal heat generation within the solid, and also, thermally developing flow through a semi-infinite porous medium.

Saito & De Lemos (2004) considered local thermal non-equilibrium and obtained the interfacial heat transfer coefficient for laminar flow using a single unit cell with local instantaneous transport equations.

In all of the above, only laminar flow has been considered. When treating turbulent flow in porous media, however, difficulties arise because the flow fluctuates with time and a volumetric average is applied Gray & Lee (1977). For handling such situations, a new concept called *double decomposition* has been proposed for developing a macroscopic model for turbulent transport in porous media Pedras & De Lemos (2000) Pedras & De Lemos (2001a) Pedras & De Lemos (2001c) Pedras & De Lemos (2001b) Pedras & De Lemos (2003). This methodology has been extended to non-buoyant heat transfer Rocamora & De Lemos (2000), buoyant flows by De Lemos & Braga (2003) and mass transfer by De Lemos & Mesquita (2003). Based on this same concept, De Lemos & Rocamora (2002) have developed a macroscopic turbulent energy equation for a homogeneous, rigid and saturated porous medium, considering local thermal equilibrium between the fluid and the solid matrix. A general classification of all methodologies for treating turbulent flow and heat transfer in porous media has been recently published De Lemos & Pedras (2001).

Motivated by the foregoing, this work focuses on turbulent flow through a packed bed, which represents an important configuration for efficient heat and mass transfer and suggests the use of equations governing thermal non-equilibrium involving distinct energy balances for both the solid and fluid phases. Accordingly, the use of such two-energy equation model requires an extra parameter to be determined, namely the heat transfer coefficient between the fluid and the solid. The contribution herein consists in proposing a new correlation for obtaining the interfacial heat transfer coefficient for turbulent flow in a packed bed. The bed is modeled as an infinite array of square rods and the range of Reynolds number, based on the size of the rod, is extended up to  $10^7$ .

The next sessions details the basic mathematical model, including the mean and turbulent fields for turbulent flows. Although the discussion of turbulent motion in porous media is not presented in this work the definition and concept to calculating the interfacial heat transfer coefficient for macroscopic flows are presented.

## 2. Microscopic Transport Equations

Microscopic transport equations for incompressible fluid flow in a rigid homogeneous porous medium have been already presented in the literature and for that they are here just presented (e.g. reference De Lemos & Rocamora (2002)). They read,

$$\text{Continuity: } \nabla \cdot \mathbf{u} = 0 . \quad (1)$$

$$\text{Momentum: } \rho \left[ \frac{\partial \mathbf{u}}{\partial t} + \nabla \cdot (\mathbf{u}\mathbf{u}) \right] = -\nabla p + \mu \nabla^2 \mathbf{u} . \quad (2)$$

$$\text{Energy - Fluid Phase: } (\rho c_p)_f \left\{ \frac{\partial T_f}{\partial t} + \nabla \cdot (\mathbf{u}T_f) \right\} = \nabla \cdot (k_f \nabla T_f) + S_f . \quad (3)$$

$$\text{Energy - Solid Phase (Porous Matrix): } (\rho c_p)_s \frac{\partial T_s}{\partial t} = \nabla \cdot (k_s \nabla T_s) + S_s . \quad (4)$$

where the subscripts  $f$  and  $s$  refer to fluid and solid phases, respectively. Here,  $\rho$  is the fluid density,  $\mathbf{u}$  is the fluid instantaneous velocity,  $p$  is the pressure,  $\mu$  represents the fluid viscosity,  $T$  is the temperature  $k_f$  is the fluid thermal conductivity,  $k_s$  is the solid thermal conductivity,  $c_p$  is the specific heat and  $S$  is the heat generation term. If there is no heat generation either in the solid or in the fluid, one has further  $S_f = S_s = 0$ .

## 3. Decomposition of Flow Variables in Space and Time

Macroscopic transport equations for turbulent flow in a porous medium are obtained through the simultaneous application of time and volume average operators over a generic fluid property  $\varphi$  Gray & Lee (1977). Such concepts are mathematically defined as,

$$\bar{\varphi} = \frac{1}{\Delta t} \int_t^{t+\Delta t} \varphi dt , \text{ with } \varphi = \bar{\varphi} + \varphi' \quad (5)$$

$$\langle \varphi \rangle^i = \frac{1}{\Delta V_f} \int_{\Delta V_f} \varphi dV ; \langle \varphi \rangle^v = \phi \langle \varphi \rangle^i ; \phi = \frac{\Delta V_f}{\Delta V} , \text{ with } \varphi = \langle \varphi \rangle^i + \varphi^i \quad (6)$$

where  $\Delta V_f$  is the volume of the fluid contained in a Representative Elementary Volume (REV)  $\Delta V$ .

The *double decomposition* idea first introduced and fully described in Pedras & De Lemos (2000) Pedras & De Lemos (2001a) Pedras & De Lemos (2001c) Pedras & De Lemos (2001b) Pedras & De Lemos (2003), combines Eqs. (5)-(6) and can be summarized as:

$$\overline{\langle \varphi \rangle^i} = \langle \bar{\varphi} \rangle^i ; \overline{\varphi^i} = \bar{\varphi}^i ; \langle \varphi^i \rangle^i = \langle \varphi \rangle^i \quad (7)$$

and,

$$\left. \begin{array}{l} \varphi' = \langle \varphi^i \rangle^i + \varphi'^i \\ \varphi^i = \bar{\varphi}^i + \varphi'^i \end{array} \right\} \text{ where } \varphi'^i = \varphi^i - \langle \varphi^i \rangle^i = \varphi^i - \bar{\varphi}^i . \quad (8)$$

Therefore, the quantity  $\varphi$  can be expressed by either,

$$\varphi = \overline{\langle \varphi \rangle^i} + \langle \varphi \rangle^i + \bar{\varphi}^i + \varphi'^i , \quad (9)$$

or

$$\varphi = \langle \bar{\varphi} \rangle^i + \bar{\varphi}^i + \langle \varphi^i \rangle^i + \varphi'^i . \quad (10)$$

The term  $\varphi'^i$  can be viewed as either the temporal fluctuation of the spatial deviation or the spatial deviation of the temporal fluctuation of the quantity  $\varphi$ .

## 4. Macroscopic Flow and Energy Equations

When the average operators (5)-(6) are applied over Eqs. (1)-(2), macroscopic equations for turbulent flow are obtained. Volume integration is performed over a Representative Elementary Volume (REV), Gray & Lee (1977) and Slattery (1967) resulting in,

$$\text{Continuity: } \nabla \cdot \bar{\mathbf{u}}_D = 0. \quad (11)$$

where,  $\bar{\mathbf{u}}_D = \phi \langle \bar{\mathbf{u}} \rangle^i$  and  $\langle \bar{\mathbf{u}} \rangle^i$  identifies the intrinsic (liquid) average of the time-averaged velocity vector  $\bar{\mathbf{u}}$ .

Momentum:

$$\rho \left[ \frac{\partial \bar{\mathbf{u}}_D}{\partial t} + \nabla \cdot \left( \frac{\bar{\mathbf{u}}_D \bar{\mathbf{u}}_D}{\phi} \right) \right] = -\nabla (\phi \langle \bar{p} \rangle^i) + \mu \nabla^2 \bar{\mathbf{u}}_D - \nabla \cdot (\rho \phi \langle \bar{\mathbf{u}}' \bar{\mathbf{u}}' \rangle^i) - \left[ \frac{\mu \phi}{K} \bar{\mathbf{u}}_D + \frac{c_F \phi \rho |\bar{\mathbf{u}}_D| \bar{\mathbf{u}}_D}{\sqrt{K}} \right], \quad (12)$$

where the last two terms in Eq. (12), represent the Darcy and Forchheimer contributions by Forchheimer (1901). The symbol  $K$  is the porous medium permeability,  $c_F$  is the form drag or Forchheimer coefficient,  $\langle \bar{p} \rangle^i$  is the intrinsic average pressure of the fluid, and  $\phi$  is the porosity of the porous medium.

The macroscopic Reynolds stress  $-\rho \phi \langle \bar{\mathbf{u}}' \bar{\mathbf{u}}' \rangle^i$  appearing in Eq. (12) is given as,

$$-\rho \phi \langle \bar{\mathbf{u}}' \bar{\mathbf{u}}' \rangle^i = \mu_{t_\phi} 2 \langle \bar{\mathbf{D}} \rangle^v - \frac{2}{3} \phi \rho \langle k \rangle^i \mathbf{I}, \quad (13)$$

where,

$$\langle \bar{\mathbf{D}} \rangle^v = \frac{1}{2} \left[ \nabla (\phi \langle \bar{\mathbf{u}} \rangle^i) + [\nabla (\phi \langle \bar{\mathbf{u}} \rangle^i)]^T \right], \quad (14)$$

is the macroscopic deformation tensor,  $\langle k \rangle^i = \langle \bar{\mathbf{u}}' \cdot \bar{\mathbf{u}}' \rangle^i / 2$  is the intrinsic turbulent kinetic energy, and  $\mu_{t_\phi}$ , is the turbulent viscosity, which is modeled in De Lemos & Pedras (2001) similarly to the case of clear flow, in the form,

$$\mu_{t_\phi} = \rho c_\mu \frac{\langle k \rangle^i}{\langle \varepsilon \rangle^i}, \quad (15)$$

The intrinsic turbulent kinetic energy per unit mass and its dissipation rate are governed by the following equations,

$$\rho \left[ \frac{\partial}{\partial t} (\phi \langle k \rangle^i) + \nabla \cdot (\bar{\mathbf{u}}_D \langle k \rangle^i) \right] = \nabla \cdot \left[ \left( \mu + \frac{\mu_{t_\phi}}{\sigma_k} \right) \nabla (\phi \langle k \rangle^i) \right] - \rho \langle \bar{\mathbf{u}}' \bar{\mathbf{u}}' \rangle^i : \nabla \bar{\mathbf{u}}_D + c_k \rho \frac{\phi \langle k \rangle^i |\bar{\mathbf{u}}_D|}{\sqrt{K}} - \rho \phi \langle \varepsilon \rangle^i. \quad (16)$$

$$\rho \left[ \frac{\partial}{\partial t} (\phi \langle \varepsilon \rangle^i) + \nabla \cdot (\bar{\mathbf{u}}_D \langle \varepsilon \rangle^i) \right] = \nabla \cdot \left[ \left( \mu + \frac{\mu_{t_\phi}}{\sigma_\varepsilon} \right) \nabla (\phi \langle \varepsilon \rangle^i) \right] + c_1 \left( -\rho \langle \bar{\mathbf{u}}' \bar{\mathbf{u}}' \rangle^i : \nabla \bar{\mathbf{u}}_D \right) \frac{\langle \varepsilon \rangle^i}{\langle k \rangle^i} + c_2 c_k \rho \frac{\phi \langle \varepsilon \rangle^i |\bar{\mathbf{u}}_D|}{\sqrt{K}} - c_2 \rho \phi \frac{\langle \varepsilon \rangle^i}{\langle k \rangle^i}. \quad (17)$$

where,  $c_k$ ,  $c_1$ ,  $c_2$  and  $c_\mu$  are non-dimensional constants.

Similarly, macroscopic energy equations are obtained for both fluid and solid phases by applying time and volume average operators to Eqs. (3)- (4). As in the flow case, volume integration is performed over a Representative Elementary Volume (REV) resulting in,

$$\begin{aligned} (\rho c_p)_f \left[ \frac{\partial \phi \langle \bar{T}_f \rangle^i}{\partial t} + \nabla \cdot \left\{ \phi \left( \langle \bar{\mathbf{u}} \rangle^i \langle \bar{T}_f \rangle^i + \langle \bar{\mathbf{u}}^i \bar{T}_f \rangle^i + \langle \bar{\mathbf{u}}' T_f' \rangle^i \right) \right\} \right] &= \nabla \cdot \left[ k_f \nabla (\phi \langle \bar{T}_f \rangle^i) \right] + \\ \nabla \cdot \left[ \frac{1}{\Delta V} \int_{A_i} \mathbf{n}_i k_f \bar{T}_f dA \right] &+ \frac{1}{\Delta V} \int_{A_i} \mathbf{n}_i \cdot k_f \nabla \bar{T}_f dA, \end{aligned} \quad (18)$$

$$(\rho c_p)_s \left[ \frac{\partial (1-\phi) \langle \bar{T}_s \rangle^i}{\partial t} \right] = \nabla \cdot \left\{ k_s \nabla [(1-\phi) \langle \bar{T}_s \rangle^i] \right\} - \nabla \cdot \left[ \frac{1}{\Delta V} \int_{A_i} \mathbf{n}_i k_s \bar{T}_s dA \right] - \frac{1}{\Delta V} \int_{A_i} \mathbf{n}_i \cdot k_s \nabla \bar{T}_s dA, \quad (19)$$

where  $\langle \bar{T}_s \rangle^i$  and  $\langle \bar{T}_f \rangle^i$  denote the intrinsically averaged temperature of solid and fluid phases, respectively,  $A_i$  is the interfacial area within the REV and  $\mathbf{n}_i$  is the unit vector normal to the fluid-solid interface, pointing from the fluid towards the solid phase. Eqs. (18) and (19) are the macroscopic energy equations for the fluid and the porous matrix (solid), respectively.

Further, using the *double decomposition* concept, Rocamora & De Lemos (2000) have shown that the fourth term on the left hand side of Eq. (18) can be expressed as:

$$\langle \bar{\mathbf{u}}' T_f' \rangle^i = \langle (\langle \bar{\mathbf{u}} \rangle^i + \langle \bar{\mathbf{u}}' \rangle^i) (\langle \bar{T}_f \rangle^i + \langle T_f' \rangle^i) \rangle^i = \langle \bar{\mathbf{u}} \rangle^i \langle \bar{T}_f \rangle^i + \langle \bar{\mathbf{u}}' \rangle^i \langle T_f' \rangle^i. \quad (20)$$

Therefore, in view of Eq. (20), Eq. (18) can be rewritten as:

$$\begin{aligned}
 (\rho c_p)_f \left[ \frac{\partial \phi \langle \overline{T_f} \rangle^i}{\partial t} + \nabla \cdot \left\{ \phi \left( \langle \overline{\mathbf{u}} \rangle^i \langle \overline{T_f} \rangle^i + \langle \overline{\mathbf{u}'} \rangle^i \langle \overline{T_f} \rangle^i + \langle \overline{\mathbf{u}} \rangle^i \langle \overline{T_f'} \rangle^i + \langle \overline{\mathbf{u}'} \rangle^i \langle \overline{T_f'} \rangle^i \right) \right\} \right] = \\
 \nabla \cdot \left[ k_f \nabla \left( \phi \langle \overline{T_f} \rangle^i \right) \right] + \nabla \cdot \left[ \frac{1}{\Delta V} \int_{A_i} \mathbf{n}_i k_f \overline{T_f} dA \right] + \frac{1}{\Delta V} \int_{A_i} \mathbf{n}_i \cdot k_f \nabla \overline{T_f} dA .
 \end{aligned} \tag{21}$$

## 5. Interfacial Heat Transfer Coefficient

In Eqs. (19) and (21) the heat transferred between the two phases can be modeled by means of a film coefficient  $h_i$  such that,

$$h_i a_i \left( \langle \overline{T_s} \rangle^i - \langle \overline{T_f} \rangle^i \right) = \frac{1}{\Delta V} \int_{A_i} \mathbf{n}_i \cdot k_f \nabla \overline{T_f} dA = \frac{1}{\Delta V} \int_{A_i} \mathbf{n}_i \cdot k_s \nabla \overline{T_s} dA . \tag{22}$$

where,  $h_i$  is known as the interfacial convective heat transfer coefficient and  $a_i = A_i/\Delta V$  is the surface area per unit volume and  $A_i$  is the interfacial heat transfer area.

Wakao *et al.* (1979) obtained a heuristic correlation for closely packed bed, of particle diameter  $D$  and compared their with experimental data. This correlation for the interfacial heat transfer coefficient is given by,

$$\frac{h_i D}{k_f} = 2 + 1.1 Re_D^{0.6} Pr^{1/3} . \tag{23}$$

For determining  $h_i$ , Kuwahara *et al.* (2001) modeled a porous medium by considering an infinite number of solid square rods of size  $D$ , arranged in a regular triangular pattern (see Fig. (1)). They numerically solved the governing equations in the void region, exploiting to advantage the fact that for an infinite and geometrically ordered medium a repetitive cell can be identified. Periodic boundary conditions were then applied for obtaining the temperature distribution under fully developed flow conditions. A numerical correlation for the interfacial convective heat transfer coefficient was proposed by Kuwahara *et al.* (2001) as,

$$\frac{h_i D}{k_f} = \left( 1 + \frac{4(1-\phi)}{\phi} \right) + \frac{1}{2} (1-\phi)^{1/2} Re_D Pr^{1/3} , \text{ valid for } 0.2 < \phi < 0.9 , \tag{24}$$

Eq. (24) is based on porosity dependency and is valid for packed beds of particle diameter  $D$ .

This same physical model will be used here for obtaining the interfacial heat transfer coefficient  $h_i$  for macroscopic flows.

Saito & De Lemos (2004) obtained the interfacial heat transfer coefficient for laminar flows through an infinite square rod; this same physical model will be used here for obtaining the interfacial heat transfer coefficient  $h_i$  for turbulent flows.

The flow through an infinite square rod can be associated with flow across bundle of tubes, furthermore the heat transfer coefficient related with a tube is determined by its position in the package. The tube rows of a bundle are either aligned or staggered in the direction of the fluid velocity. In this work the geometric arrangement is staggered (see Fig. (1)). For the staggered configuration Zhukauskas (1972) has proposed a correlation of the form,

$$\frac{h_i D}{k_f} = 0.022 Re_D^{0.84} Pr^{0.36} , \tag{25}$$

where the values 0.022 and 0.84 are constants for tube bank in cross flow and for this particular case  $2 \times 10^5 < Re_D < 2 \times 10^6$ .

## 6. Periodic Cell and Boundary Conditions

The macroscopic hydrodynamic and thermodynamic behavior of practical interest can be obtained from the direct application of the first principles to viscous flow and heat transfer at a pore scale. In reality, however, it is impossible to resolve the details of the flow and heat transfer fields within a real porous medium Nakayama *et al.* (2001) and Kuwahara *et al.* (2001) modeled a porous medium in terms of obstacles arranged in regular pattern, and solved the set of the microscopic governing equations, exploiting periodic boundary conditions. Moreover, the main objective of this research is, in fact, to enhance the reliability of the numerical results with respect to those obtained from experiments and one step forward to this direction is the formulation of the two-equation model for turbulent flows.

In order to evaluate the numerical tool to be used in the determination of the film coefficient given by Eq. (22), a test case was run for obtaining the flow field in a periodic cell, which is here assumed to represent the porous medium.

Consider a macroscopically uniform flow through an infinite number of square rods of lateral size  $D$ , placed in a staggered arrangement and maintained at constant temperature  $T_w$ . The periodic cell or representative elementary volume,  $\Delta V$ , is schematically showed in Fig. (1) and has dimensions  $2H \times H$ . Computations within this cell were carried out using a non-uniform grid, as shown in Fig. (2), to ensure that the results were grid independent. The Reynolds number  $Re_D = \rho \bar{u}_D D / \mu$  was varied from 104 to 107 and the porosity,  $\phi = 1 - (D/H)^2$ .

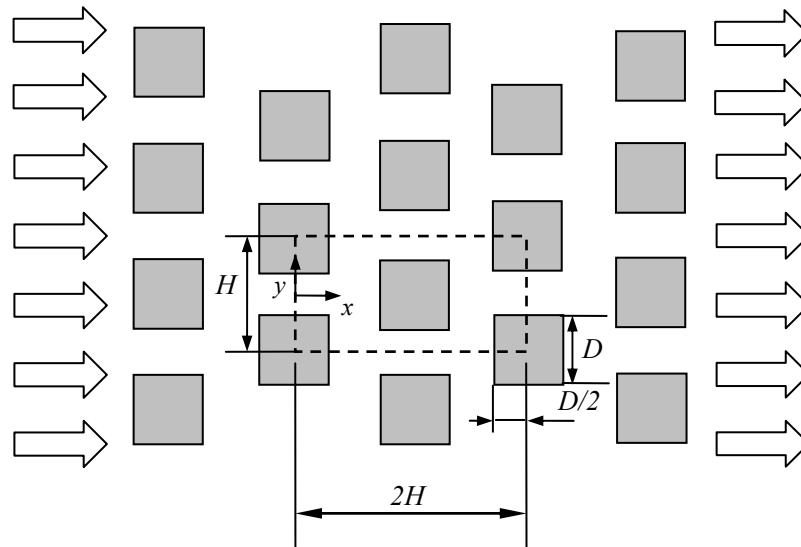


Figure 1. Physical model and coordinate system.

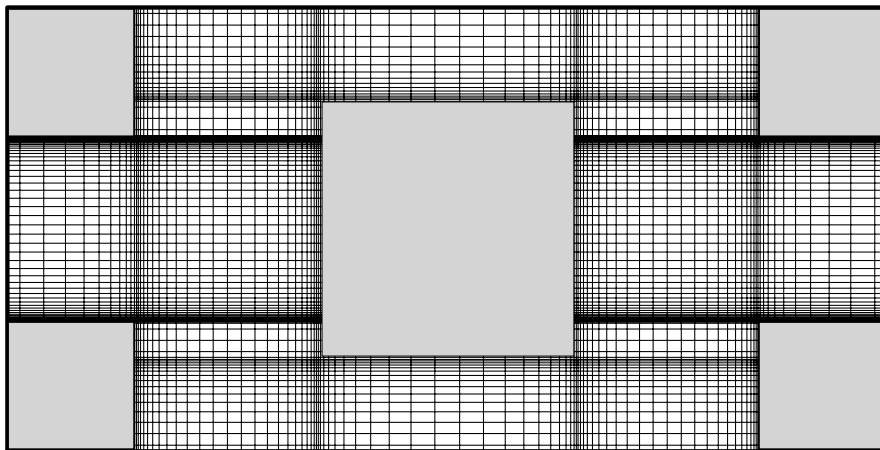


Figure 2. Non uniform computational grid.

The numerical method utilized to discretize the flow and energy equations in the unit cell is the Finite Control Volume approach. The SIMPLE method of Patankar (1980) was used for the velocity-pressure coupling. Convergence was monitored in terms of the normalized residue for each variable. The maximum residue allowed for convergence check was set to  $10^{-9}$ , being the variables normalized by appropriate reference values.

For fully developed flow in the cell of Fig. (1), the velocity at exit ( $x/H = 2$ ) must be identical to that at the inlet ( $x/H = 0$ ). Temperature profiles, however, are only identical at both cell exit and inlet if presented in terms of an appropriate non-dimensional variable. The situation is analogous to the case of forced convection in a channel with isothermal walls. Thus, boundary conditions and periodic constraints are given by:

Thus, boundary conditions and periodic constraints are given by:  
 On the solid walls (Low Re):

$$\bar{u} = 0, \quad k = 0, \quad \varepsilon = \nu \frac{\partial^2 k}{\partial y^2}, \quad \bar{T} = \bar{T}_w, \quad (26)$$

On the solid walls (high Re):

$$\frac{\bar{u}}{u_\tau} = \frac{1}{\kappa} \ln(y^+ E), \quad k = \frac{u_\tau^2}{c_\mu^{1/2}}, \quad \varepsilon = \frac{c_\mu^{3/4} k_w^{3/2}}{\kappa y_w}, \quad q_w = \frac{(\rho c_p)_f c_\mu^{1/4} k_w^{1/2} (\bar{T} - T_w)}{\left( \frac{Pr_t}{\kappa} \ln(y_w^+) + c_Q(Pr) \right)} \quad (27)$$

where,  $u_\tau = \left( \frac{\tau_w}{\rho} \right)^{1/2}$ ,  $y_w^+ = \frac{y_w u_\tau}{\nu}$ ,  $c_Q = 12.5 Pr^{2/3} + 2.12 \ln(Pr) - 5.3$  for  $Pr > 0.5$

where,  $Pr$  and  $Pr_t$  are Prandtl and turbulent Prandtl number, respectively,  $q_w$  is wall heat flux,  $u_\tau$  is wall-friction velocity,  $y_w$  is the coordinate normal to wall,  $\kappa$  is constant for turbulent flow past smooth impermeable walls or von Kármán's constant and  $E$  is an integration constant that depends on the roughness of the wall. For smooth walls with constant shear stress  $E = 9$ .

On the symmetry planes:

$$\frac{\partial \bar{u}}{\partial y} = \frac{\partial \bar{v}}{\partial y} = \frac{\partial k}{\partial y} = \frac{\partial \varepsilon}{\partial y} = 0, \quad (28)$$

where  $\bar{u}$  and  $\bar{v}$  are components of  $\bar{\mathbf{u}}$ .

On the periodic boundaries:

$$\bar{u}|_{inlet} = \bar{u}|_{outlet}, \quad \bar{v}|_{inlet} = \bar{v}|_{outlet}, \quad k|_{inlet} = k|_{outlet}, \quad \varepsilon|_{inlet} = \varepsilon|_{outlet}, \quad (29)$$

$$\theta|_{inlet} = \theta|_{outlet} \Leftrightarrow \frac{\bar{T} - \bar{T}_w}{\bar{T}_B(x) - \bar{T}_w}|_{inlet} = \frac{\bar{T} - \bar{T}_w}{\bar{T}_B(x) - \bar{T}_w}|_{outlet}, \quad (30)$$

The bulk mean temperature of the fluid is given by:

$$\bar{T}_B(x) = \frac{\int \bar{u} \bar{T} dy}{\int \bar{u} dy} \quad (31)$$

Computations are based on the Darcy velocity, the length of structural unit  $H$  and the temperature difference  $(\bar{T}_B(x) - \bar{T}_w)$ , as references scales.

## 6.1 Film Coefficient $h_i$

Determination of  $h_i$  is here obtained by calculating, for the unit cell of Fig. (1), an expression given as,

$$h_i = \frac{Q_{total}}{A_i \Delta T_{ml}} \quad (32)$$

where  $A_i = 8Dx1$ . The overall heat transferred in the cell,  $Q_{total}$ , is giving by,

$$Q_{total} = (H - D) \rho \bar{u}_B c_p (\bar{T}_B|_{outlet} - \bar{T}_B|_{inlet}), \quad (33)$$

The bulk mean velocity of the fluid is given by:

$$\bar{u}_B(x) = \frac{\int \bar{u} dy}{\int dy} \quad (34)$$

and the logarithm mean temperature difference,  $\Delta T_{ml}$  is,

$$\Delta T_{ml} = \frac{(\bar{T}_w - \bar{T}_B|_{outlet}) - (\bar{T}_w - \bar{T}_B|_{inlet})}{\ln[(\bar{T}_w - \bar{T}_B|_{outlet}) / (\bar{T}_w - \bar{T}_B|_{inlet})]} \quad (35)$$

Eq. (33) represents an overall heat balance on the entire cell and associates the heat transferred to the fluid to a suitable temperature difference  $\Delta T_{ml}$ . As mentioned earlier, Eqs. (1)-(4) were numerically solved in the unit cell until conditions Eqs. (29)-(30) were satisfied.

## 7. Results and Discussion

### 7.1 Periodic Flow

Results for velocity and temperature fields were obtained for different Reynolds numbers. In order to assure that the flow was hydrodynamically and thermally developed in the periodic cell of Fig. (1), the governing equations were solved repetitively in the cell, taking the outlet profiles for  $\bar{u}$  and  $\theta$  at exit and plugging them back at inlet. In the first run, uniform velocity and temperature profiles were set at the cell entrance for  $Pr = 1$  giving  $\theta = 1$  at  $x/H = 0$ . Then, after convergence of the flow and temperature fields,  $\bar{u}$  and  $\theta$  at  $x/H = 2$  were used as inlet profiles for a second run, corresponding to solving again the flow for a similar cell beginning in  $x/H = 2$ . Similarly, a third run was carried out and again outlet results, this time corresponding to an axial position  $x/H = 4$ , were recorded. This procedure was repeated several times until  $\bar{u}$  and  $\theta$  did not differ substantially at both inlet and outlet positions.

### 7.2 Developed Flow and Temperature Fields

The expression “macroscopically developed” is used herein to account for the fact that periodic flow has been achieved at that axial position. Figures (3) show distributions of pressure, isotherms and turbulence kinetic energy in a microscopic porous structure, obtained at  $Re_D = 10^5$  for cases of  $\phi = 0.65$ . The pressure increases at the front stagnation face of the square rod and decreases drastically around the corner as can be seen from the pressure contours, Fig. (3a). The turbulence kinetic energy is high around the corner where a strong flow acceleration takes place, therefore, a strong shear layer is formed downstream of the corners, as shown in Fig. (3b). Temperature distribution pattern is shown in Fig. (3c). Colder fluid impinges on the rod left surfaces yielding strong temperature gradients on that face. Downstream the obstacles, fluid recirculation smoothes temperature gradients and deforms isotherms within the mixing region. When the Reynolds number is sufficiently high, the thermal boundary layers cover the rod surfaces indicate that convective heat transfer overwhelms thermal diffusion.

Once fully developed flow and temperature fields are achieved, for the fully developed condition ( $x > 6H$ ), bulk temperatures were calculated according to Eq. (31), at both inlet and outlet positions. They were then used to calculate  $h_i$  using Eqs. (32)-(35). Results for  $h_i$  are plotted in Fig. (4) for  $Re_D$  up to  $10^7$ . Also plotted in this figure are results computed with correlation (24) using  $\phi = 0.65$ . The figure seems to indicate that both computations show a reasonable agreement for laminar results, moreover the turbulent numerical results for low and high Re model are presented in this figure.

The numerical correlation for the interfacial convective heat transfer coefficient has proposed by Kuwahara et al. (2001) is used only for laminar flows while for turbulent results a correlation is needed that is the long term objective of the present research endeavour and results herein represent the first step towards such goal.

The Figure (5) shows the turbulent numerical results of the interfacial convective heat transfer coefficient for various porosities ( $\phi = 0.44$ ,  $\phi = 0.65$  and  $\phi = 0.90$ ), results for  $h_i$  are plotted for  $Re_D$  up to  $10^7$ . The results for  $Re_D < 2 \times 10^5$  present distinct data then  $Re_D > 2 \times 10^5$  arise due the thermal boundary layers cover the rod surfaces and the viscous effect. In order to obtain the numerical correlation for turbulent flow it was used a fit for  $Re_D/\phi$  and  $h_i$ , furthermore the quarter minimal technique it was used to determine the best correlation, as showed in Fig. (6). Thus, the following expression can be established:

$$\frac{h_i D}{k_f} = 0.08 \left( \frac{Re_D}{\phi} \right)^{0.8} Pr^{1/3}; \text{ for } 1.0 \times 10^4 < \frac{Re_D}{\phi} < 2.0 \times 10^7, \text{ valid for } 0.2 < \phi < 0.9, \quad (36)$$

The expression for interfacial convective heat transfer coefficient for turbulent flow Eq. (36) is compared with numerical results for low and high Re model in Fig (7), moreover is compared with correlations given by Eq. (23) and Eq. (25), respectively by Wakao et al. (1979) and Zhukauskas (1972). The agreement between the present correlation, other herein correlations and the numerical results can be regarded as good quality.

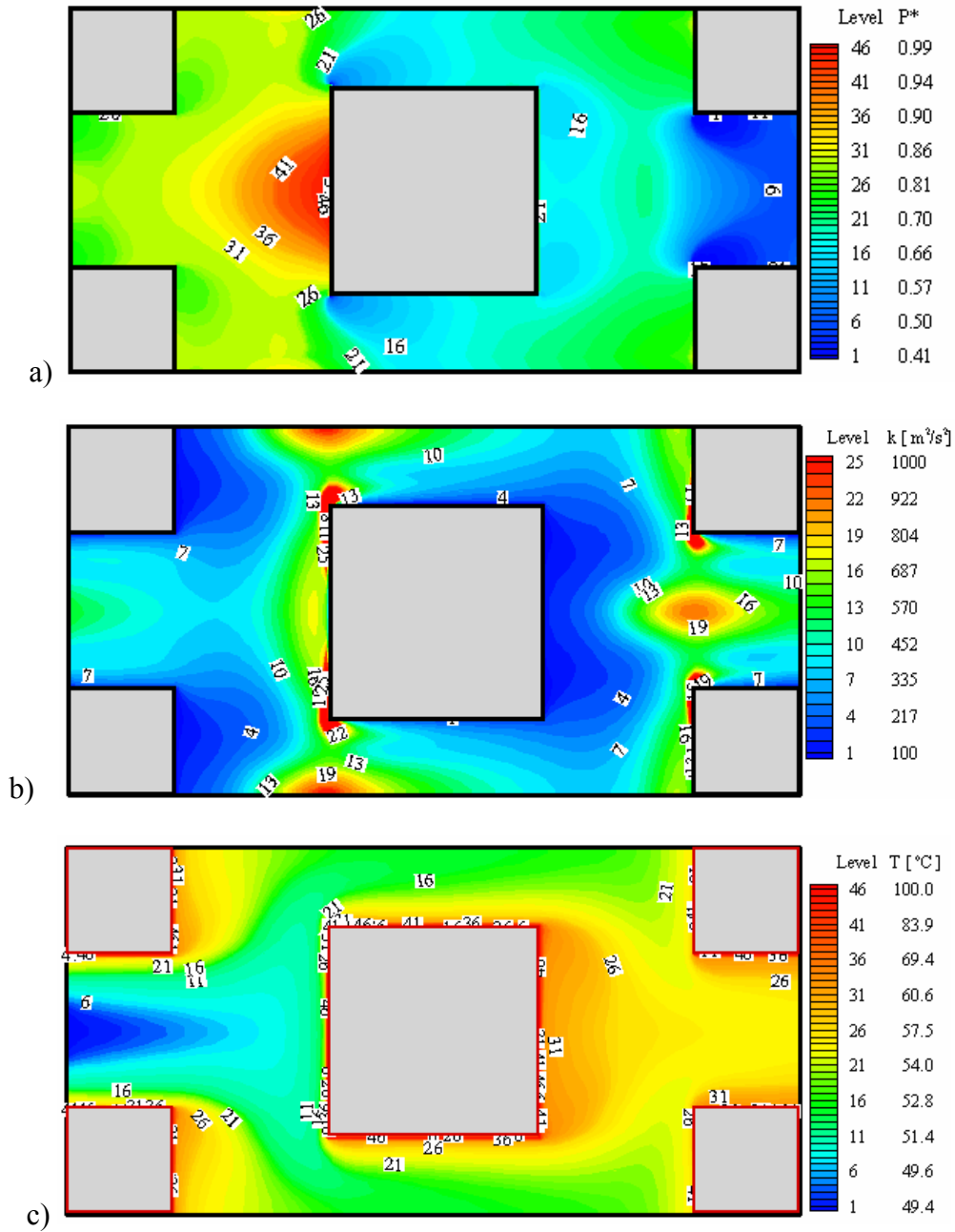


Figure 3. Square rods: (a) non-dimensional pressure; (b) turbulence kinetic energy; (c) Temperature field.

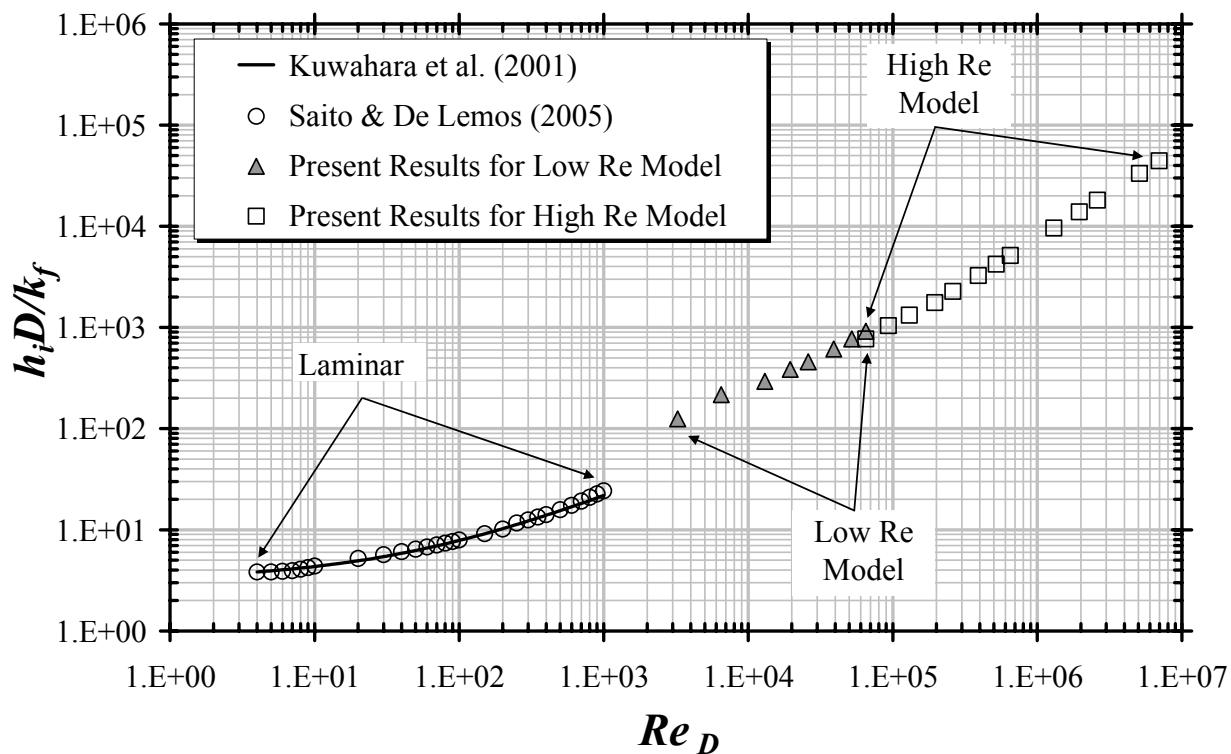


Figure 4. Effect of  $Re_D$  on  $h_i$  for  $Pr = 1$  and  $\phi = 0.65$ .

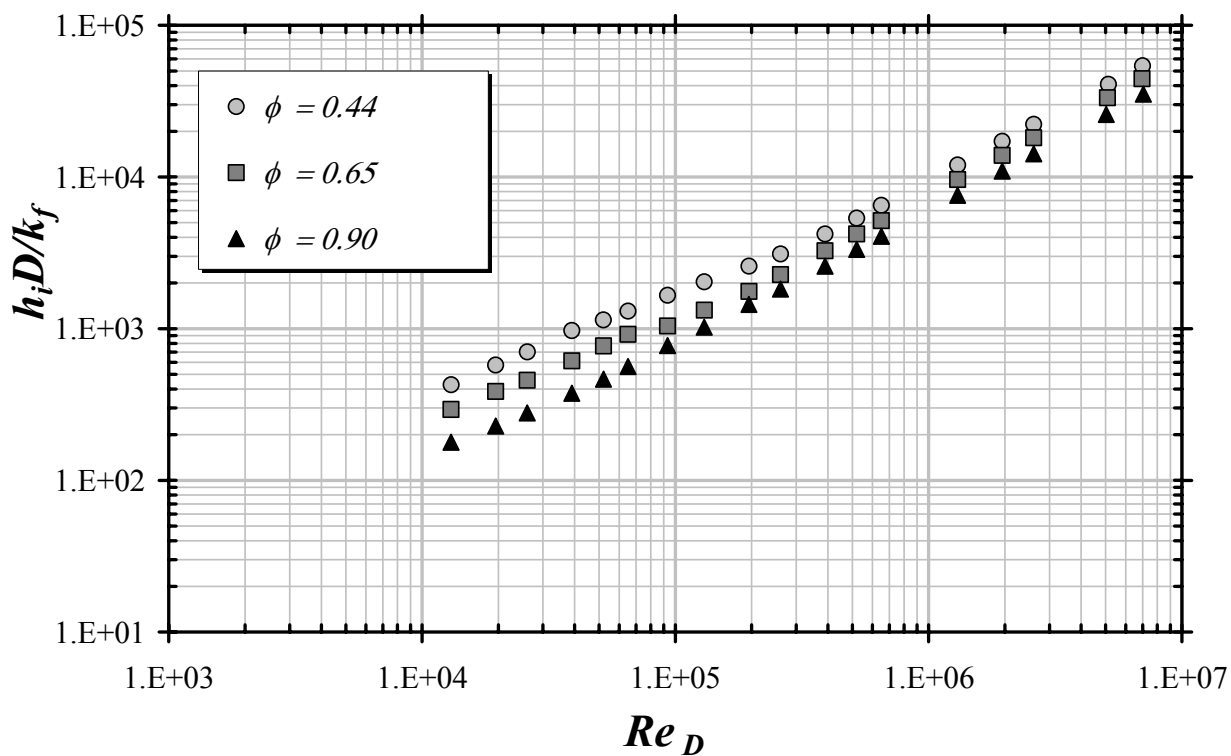


Figure 5. Effect of porosity on  $h_i$  for  $Pr = 1$ .

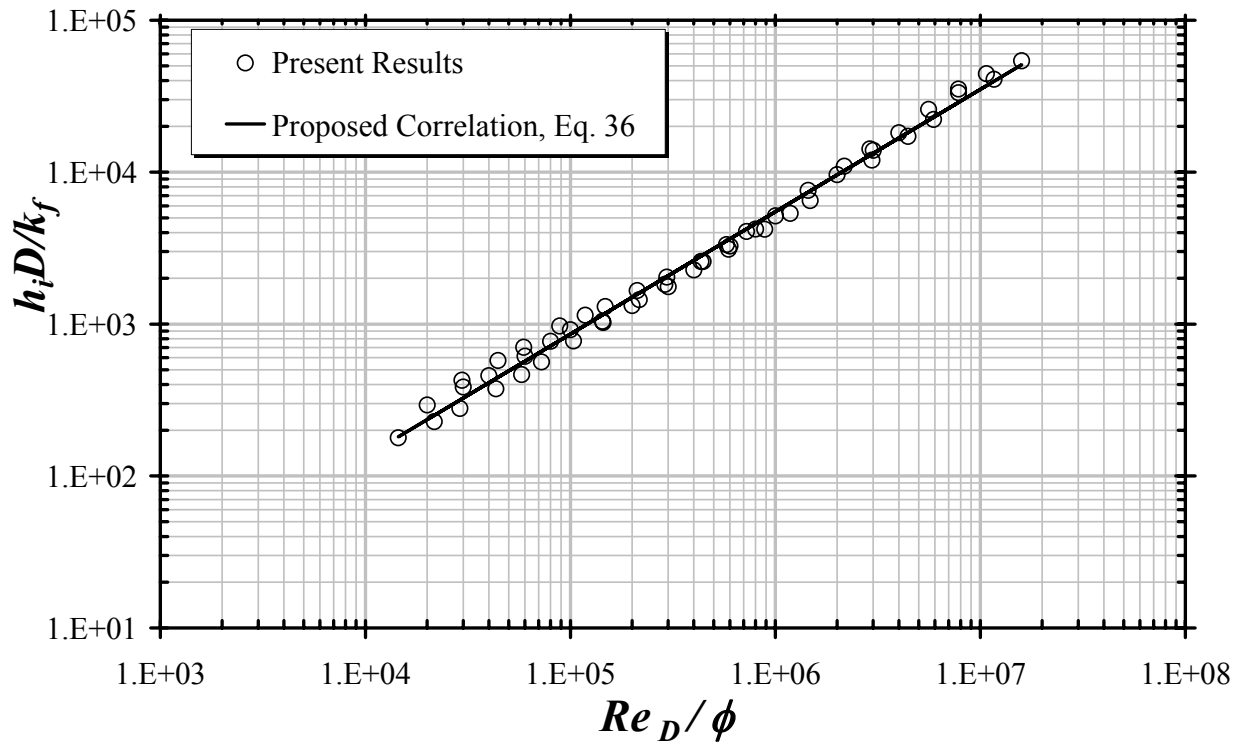


Figure 6. Comparison of the numerical results and proposed correlation.

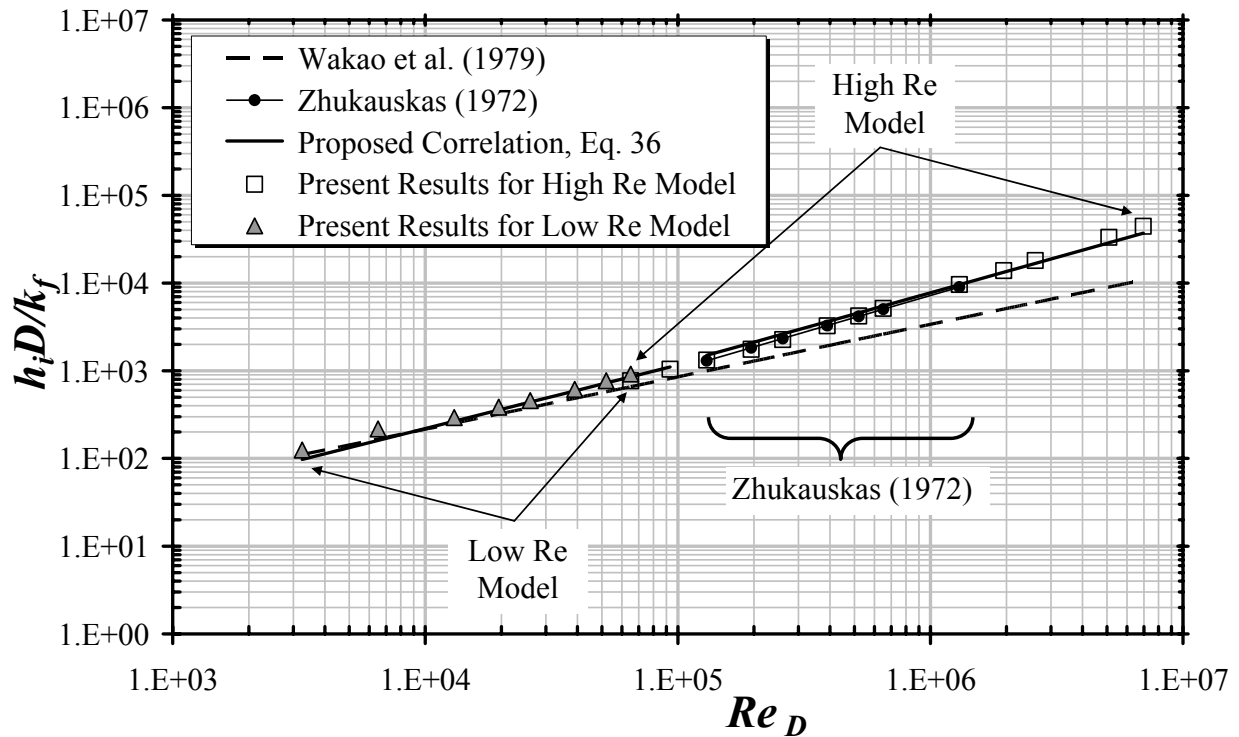


Figure 7. Comparison of the numerical results and various correlations for  $\phi = 0.65$ .

## 8. Concluding remarks

A computational procedure for determining the convective coefficient of heat exchange between the porous substrate and the working fluid for a porous medium was detailed. As a preliminary result, a macroscopically uniform laminar and turbulent flow through a periodic cell of isothermal square rods was computed, considering periodical velocity and temperature fields. Quantitative agreement was obtained when comparing the preliminary laminar results herein with simulations by Kuwahara et al. (2001) and this work obtained the heat transfer coefficient for turbulent flow using low and high Reynolds, respectively, by mean a single unit cell formed by an array of square rods. Moreover, the numerical correlation for the interfacial convective heat transfer coefficient for turbulent flow was obtained. Further work will be carried out in order to simulate fully turbulent flow and heat transfer in a porous medium formed by an array of elliptic, cylindrical and transverse elliptic rods. Besides, aligned arrangement will be analyzed. Ultimately, it is expected that a correlation for the heat transfer coefficient for turbulent flow be used in macroscopic two-energy equation model.

## 9. Acknowledgements

The authors are thankful to CNPq and FAPESP, Brazil, for their invaluable financial support during the course of this research.

## 10. References

- de Lemos, M.J.S., Pedras, M.H.J., “Recent mathematical models for turbulent flow in saturated rigid porous media”, *Journal of Fluids Engineering*, 2001, 123 (4), 935 – 940.
- de Lemos, M.J.S., Braga, E.J., “Modeling of turbulent natural convection in porous media”, *International Communications in Heat and Mass Transfer*, 2003, 30 (5), 615 – 624.
- de Lemos, M.J.S., Mesquita, M.S., “Turbulent mass transport in saturated rigid porous media”, *International Communications in Heat and Mass Transfer*, 2003, 30 (1), 105 – 115.
- de Lemos, M.J.S., Rocamora Jr, F.D., “Turbulent Transport Modeling for Heated Flow in Rigid Porous Media”, *Proc. of IHTC12 - 12th International Heat Transfer Conference, Grenoble, França, 18-23 August 2002*.
- Forchheimer, P., 1901, “Wasserbewegung durch Boden”, *Z. Ver. Deutsch. Ing.*, vol. 45, pp. 1782-1788.
- Gray, W. G. & Lee, P. C. Y., “On the theorems for local volume averaging of multiphase system”, *Int. J. Multiphase Flow*, vol. 3, pp. 333-340, 1977.
- Hsu, C.T., 1999, “A Closure Model for Transient Heat Conduction in Porous Media”, *J. Heat Transfer* 121. pp. 733-739.
- Kuwahara, F., Shirota, M., Nakayama, A., 2001, “A Numerical Study of Interfacial Convective Heat Transfer Coefficient in Two-Energy Equation Model for Convection in Porous Media”, *Int. J. Heat Mass Transfer* 44. pp. 1153-1159.
- Nakayama, A., Kuwahara, F., Sugiyama, M., Xu, G., 2001, “A Two-Energy Equation Model for Conduction and Convection in Porous Media”, *Int. J. Heat Mass Transfer* 44. pp. 4375-4379.
- Patankar, S.V., 1980, “Numerical Heat Transfer and Fluid Flow”, Mc-Graw Hill.
- Pedras, M.H.J., de Lemos, M.J.S., “On the definition of turbulent kinetic energy for flow in porous media”, *International Communications in Heat and Mass Transfer*, 2000, 27 (2), 211 – 220.
- Pedras, M.H.J., de Lemos, M.J.S., “Macroscopic turbulence modeling for incompressible flow through undeformable porous media”, *International Journal of Heat and Mass Transfer*, 2001a, 44 (6), 1081 – 1093.
- Pedras, M.H.J., de Lemos, M.J.S., “Simulation of turbulent flow in porous media using a spatially periodic array and a low Reynolds two-equation closure”, *Numerical Heat Transfer Part A – Applications*, 2001b, 39 (1).
- Pedras, M.H.J., de Lemos, M.J.S., “On the mathematical description and simulation of turbulent flow in a porous medium formed by an array of elliptic rods”, *Journal of Fluids Engineering*, 2001c, 123 (4), 941 – 947.
- Pedras, M.H.J., de Lemos, M.J.S., “Computation of turbulent flow in porous media using a Low Reynolds  $k - \epsilon$  model and an infinite array of transversally-displaced elliptic rods”, *Numerical Heat Transfer Part A – Applications*, 2003, 43 (6), 585 – 602.
- Rocamora Jr, F.D., de Lemos, M.J.S., “Analysis of convective heat transfer for turbulent flow in saturated porous media”, *International Communications in Heat and Mass Transfer*, 2000, 27 (6), 825-834.
- Saito, M.B., de Lemos, M.J.S., “Interfacial Heat Transfer Coefficient for Non-Equilibrium Convective Transport In Porous Media”, *International Communications in Heat and Mass Transfer*, vol. 32 (5), pp. 667-677 2005.
- Slattery, J. C., “Flow of viscoelastic fluids through porous media”, *A.I.Ch.E. J.*, vol. 13, pp. 1066-1071, 1967.
- Wakao, N., Kaguei, S., Funazkri, T., “Effect of fluid dispersion coefficients on particle-to-fluid heat transfer coefficients in packed bed”, *Chemical Engineering Science*, vol. 34 pp. 325-336 (1979)
- Zhukauskas, A., “Heat transfer from tubes in cross flow”, *Advances in Heat Transfer*, vol. 8, Academic Press, New York, 1972.